

An immune-responsive serpin, SRPN6, mediates mosquito defense against malaria parasites

Eappen G. Abraham*[†], Sofia B. Pinto*^{†§}, Anil Ghosh*, Dana L. Vanlandingham[¶], Aidan Budd[‡], Stephen Higgs[¶], Fotis C. Kafatos*^{§||}, Marcelo Jacobs-Lorena*^{||**}, and Kristin Michel^{‡§||**}

*Department of Molecular Microbiology and Immunology, Malaria Research Institute, Johns Hopkins Bloomberg School of Public Health, 615 North Wolfe Street, Baltimore, MD 21205; [†]European Molecular Biology Laboratory, Meyerhofstrasse 1, 69117 Heidelberg, Germany; [‡]Department of Biological Sciences, Imperial College London, Sir Alexander Fleming Building, South Kensington Campus, London SW7 2AZ, United Kingdom; [¶]Department of Pathology, University of Texas Medical Branch, Galveston, TX 77550

Contributed by Fotis C. Kafatos, September 23, 2005

We have functionally analyzed the orthologous *SRPN6* genes from *Anopheles stephensi* and *Anopheles gambiae* using phylogenetic, molecular, reverse genetic, and cell biological tools. The results strongly implicate *SRPN6* in the innate immune response against *Plasmodium*. This gene belongs to a mosquito-specific gene cluster including three additional *Anopheles* serpins. *SRPN6* expression is induced by *Escherichia coli* and both rodent and human malaria parasites. The gene is specifically expressed in midgut cells invaded by *Plasmodium* ookinetes and in circulating and attached hemocytes. Knockdown of *SRPN6* expression by RNA interference in susceptible *An. stephensi* leads to substantially increased parasite numbers, whereas depletion in susceptible *An. gambiae* delays progression of parasite lysis without affecting the number of developing parasites. However, the *An. gambiae* *SRPN6* knockdown increases the number of melanized parasites in the L3-5 refractory strain and in susceptible G3 mosquitoes depleted of *CTL4*. These results indicate that *AsSRPN6* is involved in the parasite-killing process, whereas *AgSRPN6* acts on parasite clearance by inhibiting melanization and/or promoting parasite lysis. We propose that these observed phenotypic differences are due to changed roles of the respective target serine proteases in the two mosquito species.

Anopheles | innate immunity | *Plasmodium* | midgut invasion | ookinete

Malaria is one of the most devastating infectious diseases, with 550 million cases every year (1). The causative agents of malaria are protozoan *Plasmodium* parasites, transmitted to humans exclusively by anopheline mosquito vectors. In the mosquito midgut lumen, *Plasmodium* gametocytes differentiate into gametes. After fertilization, the zygotes differentiate into motile ookinetes that invade the midgut epithelial cells ≈20–36 h postinfection (hpi). Upon emerging from the basal epithelial cell surface, ookinetes differentiate into oocysts, each producing thousands of sporozoites within 10 days. After release into the mosquito hemocoel, sporozoites invade the salivary glands, and the cycle is completed when the mosquito bites and inoculates a new individual with stored sporozoites.

Only a limited number of mosquito species are able to transmit *Plasmodium* parasites. Moreover, individual mosquitoes differ considerably in their permissiveness; in any mosquito, large losses of developing parasites occur, predominantly during ookinete midgut invasion (2, 3). Melanotic encapsulation and parasite lysis are two mechanisms responsible for parasite attrition during midgut invasion (4, 5). Lysis takes place as the ookinetes traverse the epithelial cells, and encapsulation begins when the ookinetes emerge from the midgut. The genetic basis for variation in mosquito permissiveness to parasite development is not fully understood. Several mosquito immune genes respond transcriptionally to midgut invasion by malaria parasites (6, 7), but their mechanisms of action remain mostly unclear. Recent studies have demonstrated that ookinete coating with a complement-like mosquito protein (TEP1) is one mechanism by which ookinetes are lysed in mosquito midguts (8).

Using gene silencing, Osta *et al.* (9) have shown that a leucine-rich repeat protein (LRIM1) also acts as an antagonist of ookinete development, whereas two C-type lectin immune proteins (CTL4 and CTLMA2) act in the same pathway to protect the parasite. These proteins are expressed in naïve mosquitoes and are induced in the midgut (including attached hemocytes) during ookinete invasion (9). Furthermore, knockdown (KD) of *SRPN2*, the *Anopheles gambiae* orthologue of the *Drosophila* gene *Spn27A*, accelerates parasite lysis and causes melanization of the remaining ookinetes (10). The specific roles that these molecules play in mosquito–parasite interactions and the mechanisms of their regulation remain to be elucidated.

We are interested in understanding interactions between parasites and vector mosquitoes at the molecular level. Recently we identified numerous genes up-regulated in the midgut in response to *Plasmodium berghei* (6, 11, 12). One of these, *SRPN6*, a member of the serine protease inhibitor (serpin) family, is the subject of this report. Its expression is strongly induced in both *Anopheles stephensi* and *An. gambiae* midguts during ookinete invasion. *An. gambiae* (*Ag*)*SRPN6* is also induced by the presence of *Escherichia coli* in the midgut lumen. *SRPN6* KD leads to substantially increased parasite numbers in *An. stephensi*, whereas it increases the number of melanized parasites in *An. gambiae*, in both the L3-5 refractory strain and susceptible G3 mosquitoes depleted of *CTL4*. We propose that *SRPN6* acts in synergy with *CTL4* as a component of the midgut epithelial immune-response system.

Methods

Mosquito Cultures and Parasite, Bacterial, and Viral Infection. *An. stephensi* and *An. gambiae* Keele, G3, and L3-5 strains were maintained under standard conditions. The *P. berghei* ANKA strain clone 2.34, the non-gametocyte-forming strain 2.33 (13), and the GFP-CON transgenic 259cl2 strain (14) were fed to mosquitoes by using standard procedures. *Plasmodium falciparum* strain NF54 was maintained and fed to mosquitoes as described in ref. 15. *E. coli* and o'nyong-nyong (ONN) virus infections were performed according to refs. 16 and 17.

Isolation of *An. stephensi* (*As*)*SRPN6* cDNA. The *An. stephensi* midgut cDNA library (11) was screened by using EST 3108 as a probe. The remainder of the 5' coding sequence was isolated by RT-PCR of *P. berghei*-infected *An. stephensi* midgut total RNA by using a degenerate primer d*AgSRPN6*f, designed from the translation initiation region of *AgSRPN6* and primer AsR-RT (see Table 1, which is

Conflict of interest statement: No conflicts declared.

Abbreviations: *Ag*, *An. gambiae*; *As*, *An. stephensi*; hpi, hours postinfection; KD, knockdown; ONN, o'nyong-nyong; qRT-PCR, quantitative RT-PCR.

[†]E.G.A. and S.B.P. contributed equally to this work.

^{||}To whom correspondence may be addressed. E-mail: k.michel@imperial.ac.uk, mlorena@jhsph.edu, or kafatos@embl-heidelberg.de.

**M.J.-L. and K.M. contributed equally to this work.

© 2005 by The National Academy of Sciences of the USA

published as supporting information on the PNAS web site). The full coding sequence was isolated by using an overlapping PCR of the library-isolated insert and PCR amplified 5' region.

Expression Analysis. Northern analysis was performed as described in ref. 18, by using an *An. gambiae* mitochondrial rRNA probe as loading control. For semiquantitative RT-PCR, 1 μ g of total RNA was reverse-transcribed by using oligo d(T)₁₂₋₁₅. *AsSRPN6* transcript abundance was determined by using AsF-RT and AsR-RT primers (Table 1), and ribosomal protein (S7) primers (Table 1) were used for normalization. Real-time quantitative (q)RT-PCR was performed as described in ref. 10. For primer sequences, see Table 1.

Antibody Production. The *AsSRPN6* C-terminal 205 amino acids were expressed by using pET-15b or pET32b expression system (Novagen) in *E. coli*, BL21 (DE3)pLysS, and recombinant N-terminally His-tagged full-length *AgSRPN6* fusion protein was expressed by using the pETM-11 vector in *E. coli* BL21 (DE3) strain. Both proteins were used to raise polyclonal rabbit antibodies. Both antibodies were affinity-purified against recombinant *AgSRPN6*.

Immunofluorescence and Immunoblotting. *An. stephensi* and *An. gambiae* midgut sheets were prepared as described in refs. 10 and 11. Sheets were incubated with purified *AgSRPN6* antibody (1:1,000) and P28 monoclonal antibody (1:500). The following secondary antibodies (Molecular Probes) were used: Alexa-Fluor-488-labeled goat anti-rabbit IgG, 1:1,000; rhodamine-red-X-labeled goat anti-mouse IgG, 1:1,000; Alexa-Fluor-546-labeled goat anti-mouse IgG, 1:1,500; and Alexa-Fluor-546-labeled goat anti-rabbit IgG, 1:1,500. Cell nuclei were stained with DAPI (Roche Applied Science, Indianapolis). Circulating hemocytes were collected by proboscis clipping, fixed (4% paraformaldehyde, 10 min), permeabilized (0.2% Triton X-100 in PBS, 2 min), blocked (2% BSA in PBS, 1 h), and incubated with anti-*AgSRPN6* antibody and DAPI as described above. Samples were analyzed by using a Nikon Eclipse TE200 or Zeiss LSM 510 META confocal microscope. Immunoblotting of midgut sheets was performed as described in ref. 11; *AsSRPN6* antibody and HRP-linked anti-rabbit IgG (Pierce) were used at dilutions of 1:10,000 and 1:25,000, respectively. Membranes were stripped and re-incubated with actin antibody (1:500; A2066, Sigma) as loading control. For Western analysis on cell-line supernatant, 3-day-old conditioned medium of the immune-responsive hemocyte-like cell line 4A3B (19) was harvested. Blots were incubated with 1:1,000 rabbit polyclonal anti-*AgSRPN6* antibody, and 1:20,000 goat anti-rabbit horseradish-peroxidase-conjugated secondary antibody (Promega).

Double-Stranded (ds) RNA KD. pBluescript II KS was modified by inserting a T7 promoter between the XhoI and EcoRI sites (pBSII Δ T7). An *An. stephensi SRPN6* cDNA (900–1,780-bp region) was cloned into the EcoRI site between the two T7 promoters of pBSII Δ T7. *AgSRPN6* dsRNAs were produced from plasmids pll6.1 and pll6.3. To construct pll6.1 and pll6.3, primer pairs 6.1f/r and 6.3f/r (Table 1) were used to amplify the respective *AgSRPN6* cDNA fragments and cloned into the EcoRI site of pll10. *Anopheles* mosquitoes were injected with 500 ng of *SRPN6* or control GFP dsRNA according to ref. 20; *P. berghei* infections were performed 24 h (*An. stephensi*) or 4 days (*An. gambiae*) postinjection.

Phylogenetic Analysis. Phylogenetic analysis was performed as described in ref. 10 (see *Supporting Text*, which is published as supporting information on the PNAS web site).

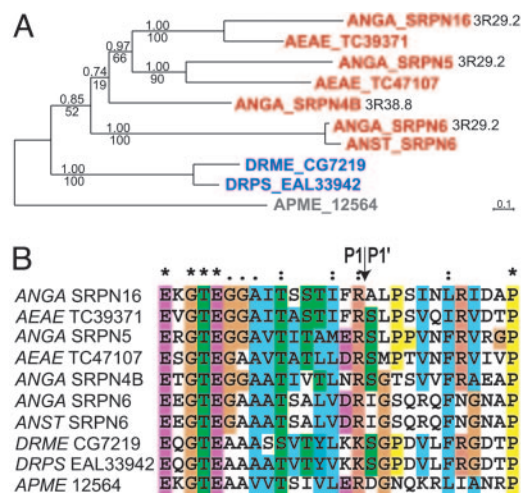


Fig. 1. Phylogenetic analysis of the *SRPN6* mosquito-specific expansion cluster. (A) Bayesian inference of phylogenetic relationships of arthropod serpins related to *SRPN6*. The *An. gambiae SRPN4*, -5, -6, and -16 form a mosquito-specific expansion cluster together with *An. stephensi SRPN6* and *Ae. aegypti* TC47107 and TC39371. Red labels correspond to mosquito, blue to drosophilid, and gray to honey bee sequences. ANGA, *An. gambiae*; ANST, *An. stephensi*; DRME, *D. melanogaster*; DRPS, *Drosophila pseudoobscura*; APME, *Apis mellifera*. Chromosomal arm (3R) locations are specified in Mb. Numbers on each branch indicate posterior probability (Upper) and bootstrap values (Lower). (B) Sequence alignment of the reactive center loops. The P1–P1' residues immediately flank the arrow (scissile bond).

Results

Isolation and Phylogenetic Analysis of *SRPN6* Genes. The *SRPN6* gene of *An. gambiae* (*AgSRPN6*), encoding a predicted protein of 494 amino acids, was identified in the annotated genome sequence (21). The corresponding *An. stephensi* gene (*AsSRPN6*) encodes a protein of 497 amino acids and was identified in a library enriched for *An. stephensi* midgut cDNAs expressed during *P. berghei* invasion and development (11, 12).

Using the BLAST program, we identified and then incorporated into a protein alignment of arthropod inhibitory serpins 10 additional *AgSRPN6*-like sequences: from GenBank, the *Aedes aegypti* gene index (www.tigr.org/tigr-scripts/tgi/T_index.cgi?species=aegypti), *Ae. aegypti* gene index), and the honey bee genome by the Ensembl genome database. Improved annotation of the honey bee serpin using GENEWISE (22) resulted in an almost full-length coding sequence. Both Bayesian Inference (BI) and Maximum Likelihood (ML) analyses of the combined alignment identified the same set of 10 sequences as clustering stably with *AgSRPN6* (results not shown). Further phylogenetic analysis of this set using both BI and ML found all of the mosquito sequences clustering together, to the exclusion of *Drosophila* and honey bee sequences, strongly suggesting an expansion of this serpin clade limited to the mosquito lineage (Fig. 1A). Additionally, *AgSRPN6* clusters stably with *AsSRPN6* (posterior probability 1.0, bootstrap 100%), clearly indicating orthology. Equally stable clustering identified two *An. gambiae*/*Aedes aegypti* pairs (*SRPN5*/*TC47107* and *SRPN16*/*TC39371*) as orthologous.

Serpins play a wide variety of roles in the physiology of many organisms (23). Each serpin interacts with its target protease via an exposed C-terminal reactive center loop (RCL), which places the so-called P1–P1' scissile bond of the reactive center in an accessible position for cleavage by the protease. The serpin then undergoes a drastic conformational change, trapping the protease in a stable complex with the inhibitor. Thus, serpins act as suicide substrates whose target specificity is determined primarily by the scissile-bond sequence. Fig. 1B compares the 28-residue RCL-loop regions of

SRPN6 and related serpins (Fig. 1A). All 10 are indeed similar, but only in *AsSRPN6* and *AgSRPN6* are they identical and have the same scissile bond, strongly indicating similar target specificities.

Ookinete Invasion Induces SRPN6. Because *AsSRPN6* is enriched in infected midgut tissues (6, 11), we analyzed in more detail the expression of *SRPN6* in both species. Using Northern analysis, we were unable to detect significant *AsSRPN6* expression at any stage during development or in adult females fed with uninfected blood (Fig. 2A) but detected strong midgut expression after feeding with blood containing gametocyte-competent, but not incompetent, *P. berghei* (Fig. 2B). This infection-specific induction was observed during the 18–48 hpi period (Fig. 2B; maximum at 30 hpi) coinciding with the period when ookinets invade the midgut epithelium. By using qRT-PCR, *SRPN6* expression was detected at low levels at all developmental stages of *An. gambiae* and was highest in adults (Fig. 2C). The apparent differences between the two species probably reflect the higher sensitivity of qRT-PCR. *AgSRPN6* expression is unaltered after a noninfective blood meal, as in *An. stephensi*, but is induced dramatically in the adult midgut after an infective *P. berghei* blood meal, maximally during the ookinete invasion period (20–24 hpi in *An. gambiae*; Fig. 2D). Interestingly, a small, 4-fold increase in *AgSRPN6* expression was also detected in mosquito carcasses during oocyst development 48 hpi (Fig. 2E).

Infection with the human malaria parasite, *P. falciparum* also induced *AsSRPN6* expression (Fig. 2F), albeit at a level significantly lower than after *P. berghei* infection (30 as compared to 25 cycles of RT-PCR). Both prevalence (30–40% vs. 90%) and intensity (0.25–0.4 vs. 121 oocysts per gut) were considerably lower for *P. falciparum* as compared to *P. berghei* infection; it is possible that *SRPN6* up-regulation increases with the number of invading ookinets.

E. coli but Not ONN Virus Induces AgSRPN6 Expression. We investigated whether other foreign organisms induce *SRPN6* expression. *E. coli* (3×10^6 per gut) fed to mosquitoes (Fig. 2G) led to a considerable increase in *AgSRPN6* expression, unlike feeding with buffer alone. No significant difference in induction was observed among mosquitoes fed on 10-, 100-, and 1,000-fold fewer bacteria; as few as 3×10^3 *E. coli* are sufficient to fully induce *SRPN6* expression (data not shown).

ONN is an alphavirus transmitted by *An. gambiae* and is usually acquired by infection of midgut epithelial cells (17). To determine whether the virus activates *SRPN6* expression, ONN-infected mosquitoes were examined by Northern analysis. No expression of *AgSRPN6* mRNA could be detected in either gut or carcass, even though hybridization of the blot with an ONN probe confirmed that the midguts were infected with virus (Fig. 2H) (24).

SRPN6 Protein Is Expressed in Infected Midgut Epithelial Cells and Hemocytes. We raised polyclonal antibodies against *As-* and *AgSRPN6* to investigate protein accumulation and localization. Immunoblot analysis of *P. berghei*-infected *An. stephensi* midgut sheet extracts detected a protein of ≈ 55 kDa at 24 and 48 hpi but not at 8 hpi, indicating that *AsSRPN6* appears at late stages of ookinete development (Fig. 3C, right lanes). Consistent with the RNA analysis, no protein was detected after a noninfective blood meal (Fig. 3C, left lanes). The affinity-purified antibody also recognized a slightly larger recombinant thioredoxin-*AgSRPN6* fusion protein and three putative degradation products ≈ 36 , 23, and 16 kDa. Consistent with this interpretation, similar-size bands were detected by Western analysis of overloaded purified recombinant SRPN6 samples (1 μ g per lane; data not shown). The SignalP (www.cbs.dtu.dk/services/SignalP/) algorithm predicted that both *As-* and *AgSRPN6* genes encode secreted proteins. Indeed, abundant *AgSRPN6* protein was detected (Fig. 3D) on Western blots of media conditioned by the immune-responsive *An. gambiae* cell line 4A3B

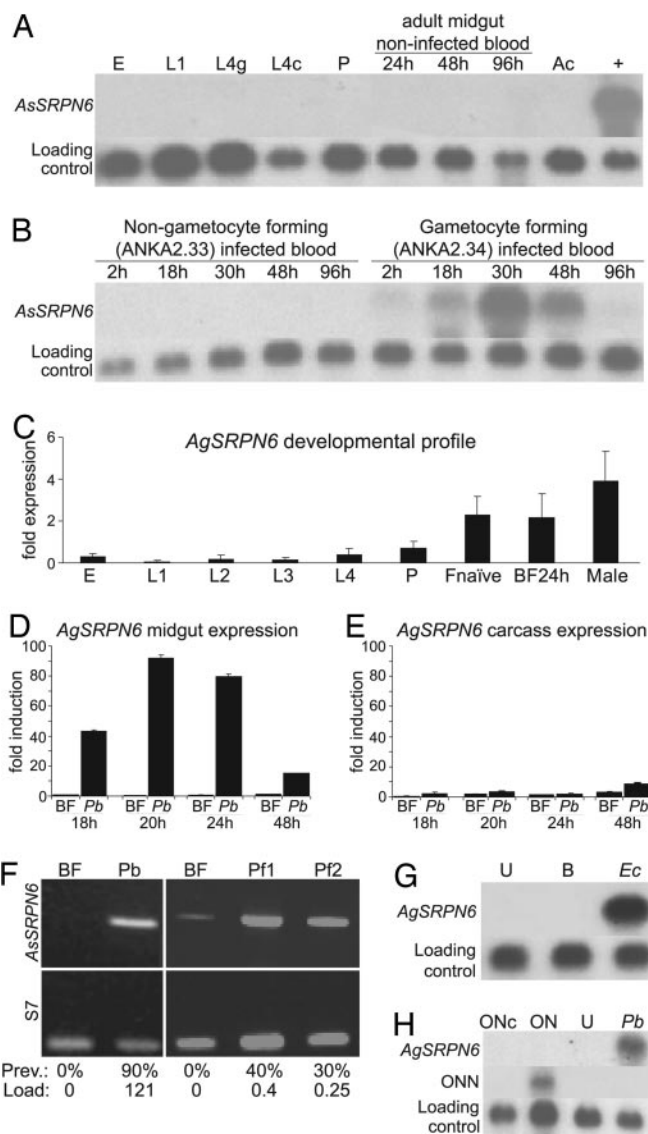


Fig. 2. *AsSRPN6* and *AgSRPN6* are strongly up-regulated by immune challenge. (A) *AsSRPN6* expression at different developmental stages and tissues and after noninfective blood meal was not detected by Northern analysis. Positive control (+): Midguts 24 h after *P. berghei* infection. (B) Northern analysis revealed strong up-regulation of *AsSRPN6* expression in midgut tissues 18–48 h after infection with gametocyte-forming *P. berghei*. (C–E) qRT-PCR analysis of *AgSRPN6* expression during development (C) and after *P. berghei* infection (D and E). Expression of *AgSRPN6* was detected mainly in adults and was strongly up-regulated in midgut tissues 20–24 h postinfection (weakly so in 48-hpi carcasses). Data were normalized to *S7* expression and calibrated to the average of all developmental stages or 18 h blood fed (BF). (F) RT-PCR analysis of *AsSRPN6* induction by *P. falciparum*. PCR amplifications were performed by using 25 cycles for *P. berghei* and 30 cycles for *P. falciparum* experiments. Prevalence and parasite load for each experiment are indicated. (Lower) Amplification of the ribosomal protein *S7* loading control. (G) Northern analysis of *An. gambiae* midgut tissue total RNA 6 h after ingestion of 3×10^5 *E. coli* or ONN virus (H) ONN virus infection was verified by using a virus-specific probe (ONN). Ac, adult carcasses; BF, blood-fed; B, buffer-fed; E, embryos; Fnaive, sugar-fed females; L1–3, first to fourth instar larvae; L4g, fourth instar guts; L4c, fourth instar carcasses; ON, ONN-infected; ONc, ONN-infected carcass; U, uninfected; P, pupae; Pb, *P. berghei*-infected; Pf1 and Pf2, *P. falciparum*-infected (two independent experiments).

(19). However, no specific bands were detected on Western analysis of hemocoel or gut-luminal contents from mosquitoes dissected at 24 or 48 hpi (data not shown). The mode and extent of extracellular SRPN6 release from cells remains to be determined.

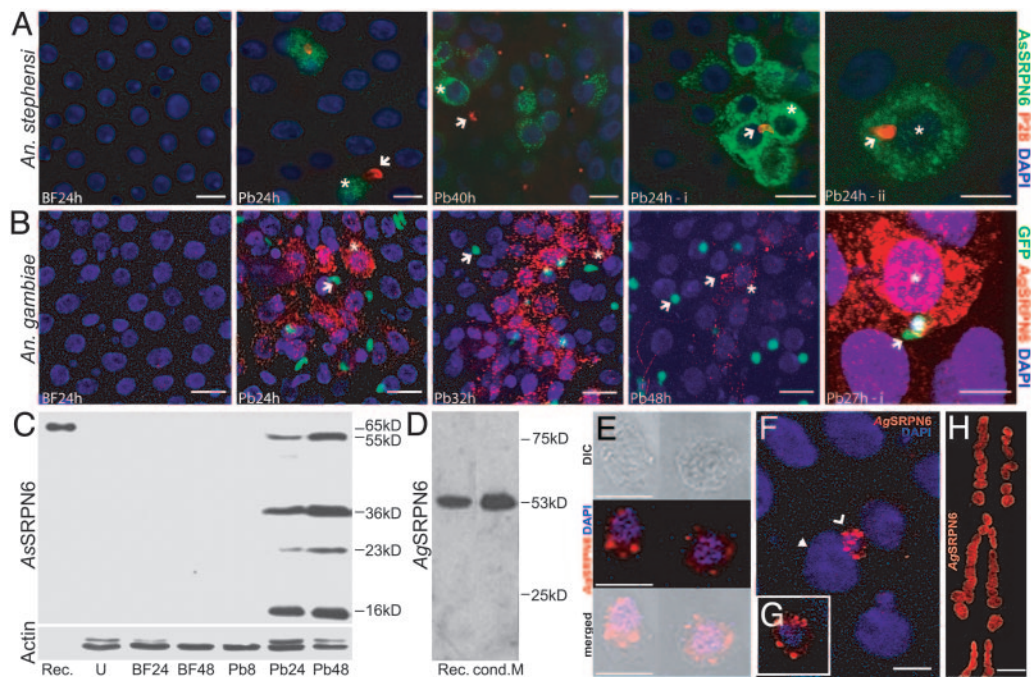


Fig. 3. Immunolocalization and immunoblotting of As- and AgSRPN6 proteins. Localization of AsSRPN6 (A) and AgSRPN6 (B) by confocal microscopy in midgut sheets at indicated time points after *P. berghei* infection (Pb). Invading parasites were mostly in close proximity or within SRPN6-positive cells (A, Pb24h-i, Pb24h-ii); the number of AgSRPN6-positive cells dropped strongly by 48 hpi. Parasites were either visualized with monoclonal anti-P28 antibody (A) or by endogenous GFP expression (B). No SRPN6 protein was detected in midgut epithelia after noninfected blood feeding (BF). Arrows indicate invading parasites. Examples of SRPN6-positive midgut epithelial cells are marked by asterisks. In A, Pb24h-ii and B, Pb27h-1, a parasite is seen emerging from a previously invaded cell, which stains intensely for SRPN6 (asterisk). (Scale bars = 10 μ m in A Pb24h-ii and Pb27h-1; all other scale bars in A and B = 20 μ m.) (C) Immunoblot of *An. stephensi* midgut sheets before (U) and after either a noninfected (BF) or *P. berghei*-infected (Pb, 90% infection prevalence, mean oocysts number 200 per gut) blood meal. Numbers after BF and Pb indicate hours after blood ingestion. The equivalent of two gut sheets was loaded per lane. Rec, 25 ng of bacterially expressed thioredoxin-AgSRPN6 fusion protein. A \approx 55-kDa protein band was detected only in infected midgut sheets. (D) AgSRPN6 protein was detected in immunoblots of conditioned medium of an *An. gambiae* cell line, indicating that the protein is secreted. Rec, 10 ng of bacterially expressed full-length AgSRPN6. (E) AgSRPN6 is expressed in circulating hemocytes. (Scale bar = 10 μ m.) (F) 30° y-plane projection of a confocal stack reveals expression of AgSRPN6 in some small-nucleated cells attached to the hemolymph-facing basal side of the midgut epithelium. Filled arrowhead, nucleus of a midgut epithelial cell; open arrowhead, a small-nucleated cell. (Scale bar = 10 μ m.) (G) Confocal slice (2 μ m) of the same cell. (H) Constitutive presence of AgSRPN6 in pericardial cells. (Scale bar = 50 μ m.)

The SRPN6 protein distribution in the midgut epithelium was investigated by immunofluorescence microscopy using antibodies to SRPN6 and P28, a major ookinete surface protein of *P. berghei* (13). As expected, neither antibody reacted with noninfected midgut sheets. In *An. stephensi* (Fig. 3A), AsSRPN6-positive cells were detected at 24 hpi, 85% of which colocalized with invading parasites; the frequency dropped to 48% at 40 hpi and 2% at 72 hpi (Table 2, which is published as supporting information on the PNAS web site). The prevalence of AsSRPN6-positive cells and invading ookinetes decreased in parallel over time, suggesting that positive cells are those invaded by parasites, as observed in the case of nitric oxid synthase and SRPN10 (25, 26). At 24 hpi, \approx 5% of single parasites were surrounded by several SRPN6-positive cells (Fig. 3A, Pb24h-i). Similar “induction clusters” have been observed previously for SRPN10 (25). In *An. gambiae*, confocal microscopy revealed a similar correlation: The number of AgSRPN6-positive cells increased from 24 to 32 h and dropped sharply thereafter. The frequency of parasites in the direct vicinity of AgSRPN6-positive cells was 57% at 24 hpi, increased to 79% at 32 h, and dropped to only 6% at 40 hpi (Table 2; see also Fig. 3B). The decrease in association between parasites and SRPN6-positive cells at later stages of infection may be due to exfoliation of SRPN6-positive cells, movement of ookinetes in the basal extracellular space after exiting the invaded cells, or degradation of SRPN6 once the parasite exits.

Confocal sections through the center of invaded midgut epithelial cells showed widespread cytoplasmic distribution of SRPN6, especially in granules (Fig. 3A, Pb24h-ii, Fig. 3B, Pb27h-i). High resolu-

tion confocal analysis also detected granules of AgSRPN6 in circulating hemocytes (Fig. 3E) and in small-nucleated cells, most likely hemocytes, attached to the basal side of the midgut facing the hemocoel (Fig. 3F and G). SRPN6 also accumulated in pericardial cells (Fig. 3H), the scavenging nephrocytes of insects, where it showed a granular cytoplasmic distribution, as described for other secreted proteins, such as Sp22D and TEP1 (27, 28).

SRPN6 Limits Malaria Parasite Infectivity to Mosquitoes. We used dsRNA-based gene silencing to investigate whether SRPN6 influences *P. berghei* development in the mosquito. Experimental or control mosquitoes were injected with SRPN6 or GFP dsRNA, respectively, followed 1 day (*An. stephensi*) or 4 days (*An. gambiae*) later by infective blood meals. RT-PCR or qRT-PCR analysis of RNA extracted 1 day postinfection showed efficient SRPN6 RNA depletion in experimental as compared to control midguts (see Fig. 5, which is published as supporting information on the PNAS web site).

KD of AsSRPN6 significantly increased the number of developing oocysts, 2.5-fold (Mann–Whitney *U* test, $P < 0.001$) in *An. stephensi* (Fig. 4A; and see Table 3, which is published as supporting information on the PNAS web site), suggesting that SRPN6 may act in a parasite-killing pathway of the type revealed by the antagonistic effects of TEP1 or LRIM on *P. berghei* in *An. gambiae* (8, 9). Surprisingly, KD of AgSRPN6 did not affect oocyst numbers in three *An. gambiae* strains susceptible to *P. berghei* infection (G3, Yaounde, and A69; Fig. 4B, Table 3). In contrast, KD increased the numbers of melanized ookinetes 2.9-fold in the refractory L3-5

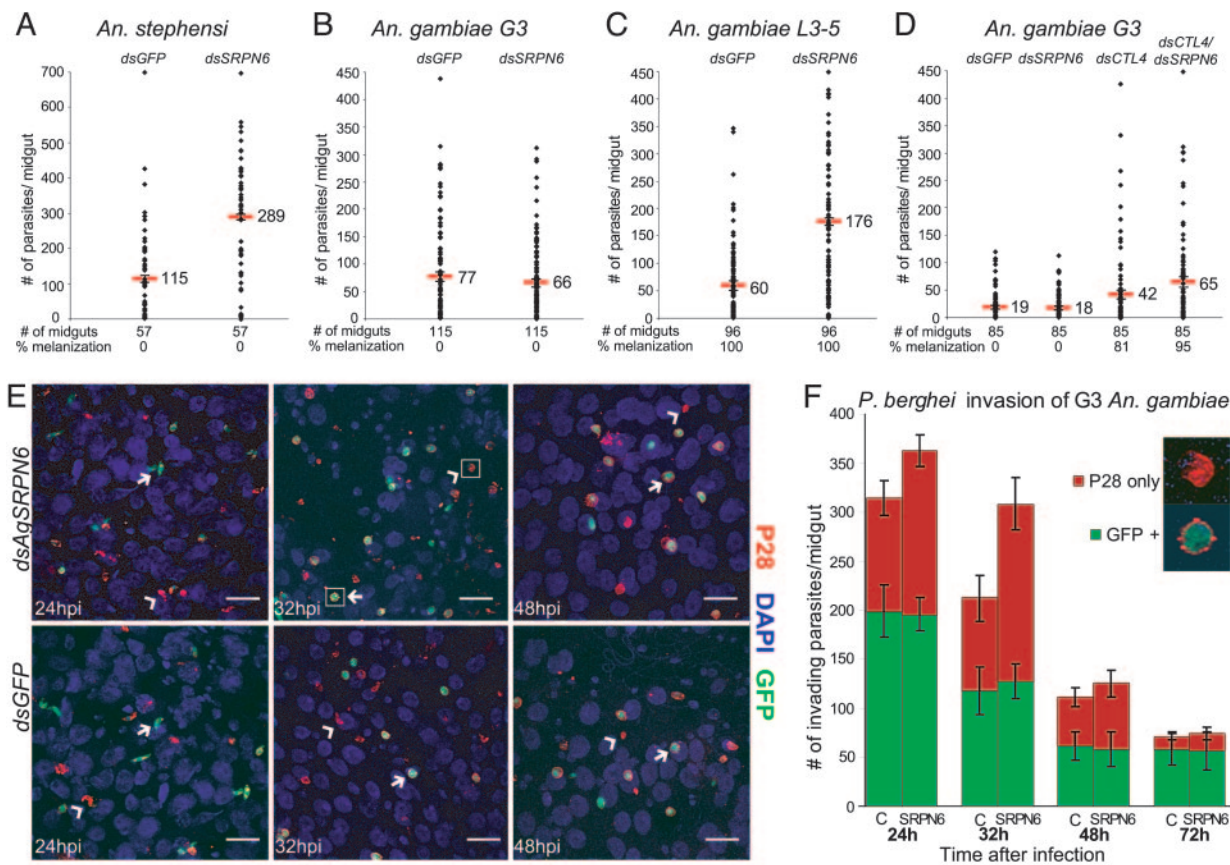


Fig. 4. Effects of *SRPN6* KD on *P. berghei* development in the mosquito. (A–D) Graphs show the distribution of overall numbers of parasites per midgut 8–15 days postinoculation in *dsSRPN6* or control *dsGFP*-treated mosquitoes. Geometric means (± 1 SE) in the pooled datasets from at least three independent experiments, the numbers of midguts examined, and the percentage of melanized parasites per midgut are indicated. See also Table 3 and Fig. 6, which is published as supporting information on the PNAS web site. The *SRPN6*-KD significantly increases the number of developing parasites in susceptible *An. stephensi* (A), but not in susceptible *An. gambiae* (B and D); the numbers of melanized parasites increase significantly in *dsSRPN6* vs. control-treated refractory L3-5 (C) and in the double-KD *CTL4/SRPN6* *An. gambiae* (D). (E) Three-dimensional projections of midguts dissected and stained with anti-P28 antibody and DAPI at indicated times after infection. Mosquitoes had been treated with either *dsAgSRPN6* or *dsGFP* 4 days before infection. Living parasites (arrows) appear green and yellow, because they are double-labeled with anti-P28 antibody (red) and endogenous GFP (green). Open arrowheads indicate P28-only parasites in the process of lysis. White squares, parasites are shown in close-up insets in F. (Scale bar = 20 μ m.) (F) Graphical representation of temporally changing parasite phenotypes detected in *dsGFP* and *dsSRPN6*-treated mosquito midguts at indicated times after infection. Bar graphs, coded as indicated in the insets, represent GFP-fluorescent live parasites (green) or lysing P28-only parasites (red). (Insets) Confocal micrographs of these two parasite classes. Error bars represent standard error in the pooled data set of three independent experiments.

strain, which melanizes ookinetes as they exit the midgut epithelium (Fig. 4C, Table 3). This increase was highly significant (Mann-Whitney *U* test, $P < 0.001$). To investigate further whether this effect depends on melanization, we altered genetically the susceptible G3 mosquitoes to a melanizing refractory phenotype by KD of *CTL4*. Consistent with previous results (9), *CTL4* KD caused melanization of 81% of invading parasites but did not significantly increase the total number of parasites. In contrast, the double-KD of *CTL4* and *AgSRPN6* increased the number of melanized parasites significantly (1.8-fold) and caused melanization of 95% of parasites (Fig. 4D; and see Table 4, which is published as supporting information on the PNAS web site). These results indicate genetic interaction, with *SRPN6* functioning as an enhancing modifier of the *CTL4*-KD melanization phenotype. Evidently, when active, these two genes cooperate in down-regulating ookinete melanization.

To investigate whether *AgSRPN6* KD has an effect on parasite lysis, we performed a separate, detailed time-course analysis of ookinete midgut invasion in G3 mosquitoes, using GFP as a marker for live parasites and P28 as a surface marker for live (P28⁺GFP⁺) parasites and for dead (P28-only) ookinetes in the process of lysis (8, 10). In accordance with data in refs. 8 and 10,

we found that, even in these susceptible mosquitoes, $\approx 80\%$ of invading ookinetes are killed and subsequently eliminated by parasite lysis during the first 72 h of infection. As expected from the above results (Fig. 4B; and see Table 5, which is published as supporting information on the PNAS web site), we did not find significant differences between control and *AgSRPN6*-KD G3 mosquitoes in the number of live (GFP⁺) parasites during the first 72 hpi (Fig. 4E and F). However, P28-only dead parasites in the process of lysis were initially more numerous after *SRPN6*-KD. This difference was maximal at 32 hpi and completely disappeared by 72 hpi, indicating that, in susceptible *An. gambiae*, KD of *AgSRPN6* transiently slows down parasite lysis.

Discussion

The *An. gambiae* serpin genes *SRPN5*, *-6*, and *-16* are clustered within 20 kb on chromosome 3. Our phylogenetic analysis indicated that this genomic proximity is the result of tandem gene duplications that occurred after the divergence of mosquitoes from drosophilids. The phylogenetic analysis also identified *An. gambiae* and *An. stephensi* *SRPN6* genes as an orthologous pair; similarly, the *An. gambiae* *SRPN5* and *-6* genes are orthologues of *Ae. aegypti* TC39371 and TC47107 sequences, respectively. This mosquito-

specific expansion led to gene-sequence diversification, possibly reflecting selection pressures to adapt to differential ecological and physiological challenges, among them hematophagy and exposure to blood-borne pathogens and parasites (21). Interestingly, *Drosophila melanogaster* CG7219 has been shown to be up-regulated after bacterial challenge (29), suggesting that an early function of this clade in dipteran innate immunity might have been elaborated after gene reduplication in mosquitoes.

SRPN6 sequences were identified as overrepresented in an *An. stephensi* subtraction library enriched for sequences expressed in the midgut of *P. berghei*-infected mosquitoes (11) and in microarray midgut invasion-specific signals from *An. gambiae* (6). Our detailed expression analysis of *SRPN6* extended these findings, firmly establishing that *SRPN6* is strongly and specifically induced during the parasites' passage through the midgut epithelium. Importantly, *AgSRPN6* is also up-regulated after infection with the human malaria parasite, *P. falciparum*. Therefore, induction seems to be independent of parasite species and host blood factors but depends on ookinete invasion: Noninvasive parasites in the blood meal do not induce *SRPN6* expression. These findings indicate that *SRPN6* expression in the mosquito midgut epithelium may depend on direct interaction of microorganisms with the midgut cell. The failure of ONN virus to induce *SRPN6* expression suggests some pathogen-specificity of this response, although a quantitative explanation cannot be excluded.

Immunolocalization experiments indicated that *SRPN6* transiently colocalizes with and near the parasites in both mosquito species. The colocalization coincides with the parasites' passage through the midgut epithelium and then subsides, suggesting transient expression combined with a short *SRPN6* half-life. Alternatively, loss of colocalization may reflect the known propensity of postinvasion ookinetes to move laterally within the subepithelial space and of invaded cells to be extruded from the epithelium (25, 30). It has been shown that a single ookinete can invade multiple midgut cells before emerging on the basal side of the epithelium (25, 30), and this fact, rather than propagated induction, may explain the observed *SRPN6*-positive cell clusters. Although no *SRPN6* protein was detected in the midgut lumen or the hemolymph at various time points after infection, the prediction of a strong signal peptide, the granular cellular distribution of *SRPN6*, and its detection in cell-line-conditioned medium strongly suggest that this serpin can be secreted. Further work is needed to distinguish between these hypotheses and to determine the extent of colocalization with additional markers within the invaded and apoptotic cells.

As *SRPN6* expression is closely linked to invasion of *P. berghei* within its mosquito vector, we examined whether this serpin indeed

has an influence on the outcome of infection. RNA interference induced by dsRNA injection led to significant *SRPN6* reduction in *An. stephensi* and *An. gambiae* midgut tissues and, importantly, affected strongly the vectorial capacity of *An. stephensi*. Similar to the KD phenotype of TEP1 and LRIM1 (8, 9), *AsSRPN6*-KD significantly increased the number of developing oocysts. In contrast, KD of *AgSRPN6* had no effect on infection prevalence or oocyst load; therefore, this serpin is not involved in parasite killing in *An. gambiae*. However, detailed cell biological analysis of the *P. berghei* midgut invasion process in *AgSRPN6*-KD mosquitoes showed an effect on clearance of dead parasites: Lysis is slowed down by this KD. Delayed lysis would make more parasites available for melanization and could, thus, explain the observed increase in numbers of melanized parasites in the CTL4/*SRPN6* double-KD and in the refractory L3-5 mosquitoes.

Blandin *et al.* (8) hypothesized that parasite elimination is a two-step process, wherein parasites are killed first, and dead parasites are subsequently cleared by lysis or become melanized, in the case of the refractory L3-5 strain. Our results suggest that *AsSRPN6* is either directly or indirectly involved in the parasite-killing process, whereas *AgSRPN6* apparently acts further downstream on parasite clearance by promoting lysis. The sequence similarity between these two orthologues and their identical hinge regions strongly indicate similar target specificities. It is, therefore, likely that the observed phenotypic differences are due to changed modes of action of the respective putative target serine proteases in the two mosquito species. Thus far, all insect serpins known to play a role in insect immunity, including *AgSRPN2*, do so by down-regulating immune pathways (10, 31–33). Interestingly, results presented here indicate that the roles of *SRPN6* differ between mosquito species, possibly subject to interactions with other genes implicated in antiparasitic responses. Future work is needed to elucidate how *SRPN6* mediates specific mosquito defenses against foreign organisms in the context of different genetic backgrounds.

We thank Dolores Doherty, Anirudh Mally, and Neil Cheddie for excellent technical support; R. E. Sinden (Imperial College London, London) for anti-P28 antibody; and A. Waters (Leiden University Medical Center, Leiden, The Netherlands) for the *P. berghei* GFP-CON strain. This work was supported by the European Molecular Biology Laboratory, grants from the National Institutes of Health, Defense Advanced Research Planning Agency Grant Cooperative Agreement N00178-02-2-9002 with the Chemical Biological Radiological Sciences and Technology Defense Branch of the Naval Surface Warfare Center (Dahlgren, VA), and the FP6 Biology and Pathology of the Malaria Parasite NoE LSHP-CT-2004-503578. K.M. was supported by a research fellowship from the German Research Foundation.

- Snow, R. W., Guerra, C. A., Noor, A. M., Myint, H. Y. & Hay, S. I. (2005) *Nature* **434**, 214–217.
- Niare, O., Markianos, K., Volz, J., Oduol, F., Toure, A., Bagayoko, M., Sangare, D., Traore, S. F., Wang, R., Blass, C., *et al.* (2002) *Science* **298**, 213–216.
- Sinden, R. E. (2002) *Cell. Microbiol.* **4**, 713–724.
- Collins, F. H., Sakai, R. K., Vernick, K. D., Paskewitz, S., Seeley, D. C., Miller, L. H., Collins, W. E., Campbell, C. C. & Gwadz, R. W. (1986) *Science* **234**, 607–610.
- Vernick, K. D., Fujioka, H., Seeley, D. C., Tandler, B., Aikawa, M. & Miller, L. H. (1995) *Exp. Parasitol.* **80**, 583–595.
- Vlachou, D., Schlegelmilch, T., Christophides, G. K. & Kafatos, F. C. (2005) *Curr. Biol.* **15**, 1–11.
- Tahar, R., Boudin, C., Thiery, I. & Bourguoin, C. (2002) *EMBO J.* **21**, 6673–6680.
- Blandin, S., Shiao, S. H., Moita, L. F., Janse, C. J., Waters, A. P., Kafatos, F. C. & Levashina, E. A. (2004) *Cell* **116**, 661–670.
- Osta, M. A., Christophides, G. K. & Kafatos, F. C. (2004) *Science* **303**, 2030–2032.
- Michel, K., Budd, A., Pinto, S., Gibson, T. J. & Kafatos, F. C. *EMBO Rep.* **6**, 891–897.
- Abraham, E. G., Islam, S., Srinivasan, P., Ghosh, A. K., Valenzuela, J. G., Ribeiro, J. M., Kafatos, F. C., Dimopoulos, G. & Jacobs-Lorena, M. (2004) *J. Biol. Chem.* **279**, 5573–5580.
- Srinivasan, P., Abraham, E. G., Ghosh, A. K., Valenzuela, J., Ribeiro, J. M., Dimopoulos, G., Kafatos, F. C., Adams, J. H., Fujioka, H. & Jacobs-Lorena, M. (2004) *J. Biol. Chem.* **279**, 5581–5587.
- Paton, M. G., Barker, G. C., Matsuoka, H., Ramesar, J., Janse, C. J., Waters, A. P. & Sinden, R. E. (1993) *Mol. Biochem. Parasitol.* **59**, 263–275.
- Frank-Fayard, B., Khan, S. M., Ramesar, J., van der Keur, M., van der Linden, R., Sinden, R. E., Waters, A. P. & Janse, C. J. (2004) *Mol. Biochem. Parasitol.* **137**, 23–33.
- Ifediba, T. & Vanderberg, J. P. (1981) *Nature* **294**, 364–366.
- Moskalyk, L. A., Oo, M. M. & Jacobs-Lorena, M. (1996) *Insect Mol. Biol.* **5**, 261–268.
- Vanlandingham, D. L., Hong, C., Klingler, K., Tsatsarkin, K., McElroy, K. L., Powers, A. M., Lehane, M. J. & Higgs, S. (2005) *Am. J. Trop. Med. Hyg.* **72**, 616–621.
- Edwards, M. J., Lemos, F. J., Donnelly-Doman, M. & Jacobs-Lorena, M. (1997) *Insect Biochem. Mol. Biol.* **27**, 1063–1072.
- Muller, H. M., Dimopoulos, G., Blass, C. & Kafatos, F. C. (1999) *J. Biol. Chem.* **274**, 11727–11735.
- Blandin, S., Moita, L. F., Kocher, T., Wilm, M., Kafatos, F. C. & Levashina, E. A. (2002) *EMBO Rep.* **3**, 852–856.
- Christophides, G. K., Zdobnov, E., Barillas-Mury, C., Birney, E., Blandin, S., Blass, C., Brey, P. T., Collins, F. H., Danielli, A., Dimopoulos, G., *et al.* (2002) *Science* **298**, 159–165.
- Birney, E., Clamp, M. & Durbin, R. (2004) *Genome Res.* **14**, 988–995.
- Gettins, P. G. (2002) *Chem. Rev.* **102**, 4751–4804.
- Sim, C., Hong, Y. S., Vanlandingham, D. L., Christophides, G. C., Kafatos, F. C., Higgs, S. & Collins, F. H. *Insect Mol. Biol.* **14**, 475–481.
- Danielli, A., Barillas-Mury, C., Kumar, S., Kafatos, F. C. & Loukeris, T. G. (2005) *Cell. Microbiol.* **7**, 181–190.
- Han, Y. S., Thompson, J., Kafatos, F. C. & Barillas-Mury, C. (2000) *EMBO J.* **19**, 6030–6040.
- Danielli, A., Loukeris, T. G., Lagueux, M., Muller, H. M., Richman, A. & Kafatos, F. C. (2000) *Proc. Natl. Acad. Sci. USA* **97**, 7136–7141.
- Levashina, E. A., Moita, L. F., Blandin, S., Vriend, G., Lagueux, M. & Kafatos, F. C. (2001) *Cell* **104**, 709–718.
- De Gregorio, E., Spellman, P. T., Rubin, G. M. & Lemaitre, B. (2001) *Proc. Natl. Acad. Sci. USA* **98**, 12590–12595.
- Vlachou, D., Zimmermann, T., Cantera, R., Janse, C. J., Waters, A. P. & Kafatos, F. C. (2004) *Cell. Microbiol.* **6**, 671–685.
- Levashina, E. A., Langley, E., Green, C., Gubb, D., Ashburner, M., Hoffmann, J. A. & Reichhart, J. M. (1999) *Science* **285**, 1917–1919.
- Ligoxygakis, P., Pelte, N., Ji, C., Leclerc, V., Duvic, B., Belvin, M., Jiang, H., Hoffmann, J. A. & Reichhart, J. M. (2002) *EMBO J.* **21**, 6330–6337.
- Zhu, Y., Wang, Y., Gorman, M. J., Jiang, H. & Kanost, M. R. (2003) *J. Biol. Chem.* **278**, 46556–46564.